Journal of Computer-Aided Molecular Design, 10 (1996) 100–106
ESCOM

J-CAMD 336

Structure–activity analysis of fluorinated 1-*N*-arylamino-1-arylmethanephosphonic acid esters as inhibitors of the NADH:ubiquinone oxidoreductase (complex I)

H. Dronia[a], U. Gruß[a], G. Hägele[a,*], T. Friedrich[b] and H. Weiss[b]

[a]*Institut für Anorganische Chemie und Strukturchemie I, Heinrich-Heine-Universität Düsseldorf, Universitätsstrasse 1, D-40225 Düsseldorf, Germany*
[b]*Institut für Biochemie, Heinrich-Heine-Universität Düsseldorf, Universitätsstrasse 1, D-40225, Düsseldorf, Germany*

Received 4 July 1995
Accepted 14 December 1995

Keywords: 1-*N*-Arylamino-1-arylmethanephosphonic acid ester; Inhibitor; NADH:Ubiquinone oxidoreductase (complex I); Molecular modelling

Summary

The structural and electronic properties of fluorinated 1-*N*-arylamino-1-arylmethanephosphonic acid esters were studied and related to the inhibitory effects on NADH:ubiquinone oxidoreductase (complex I). Electrostatic potential surfaces, dipole moments and molecular geometries were analysed. Based on the conformational analysis and the electronic parameters, a simple model for the active site of the fluorinated 1-*N*-arylamino-1-arylmethanephosphonic acid esters was developed, explaining the inhibitory power. The strongest inhibition effects were found for the 1-(*N*-4-trifluoromethoxyphenyl)-amino-1-phenylmethanephosphonic acid diethyl ester **1bab**.

Introduction

The energy-transducing NADH:ubiquinone oxidoreductase (E.C. 1.6.99.3; complex I) is part of the mitochondrial and purple bacterial respiratory chains. The complex links the transfer of electrons from NADH to ubiquinone with the translocation of protons across the membrane. One flavin mononucleotide and an up until now not exactly defined number of iron–sulfur clusters serve as prosthetic groups in this reaction [1–3]. The complex is an assembly of a large number of different polypeptide subunits. The minimal form of the complex found in bacteria consists of 14 different subunits, while the mitochondrial complex comprises 42 subunits, seven of them being encoded by mitochondrial DNA [2,4]. The interest in complex I has recently increased due to the discovery that some neurodegenerative diseases, like Parkinson's disease, may be associated with a dysfunction of the complex [1,5]. The present knowledge about the electron-transfer steps in the complex is scarce. This is due mainly to the failure of electron paramagnetic resonance (EPR) spectroscopy to resolve the fast intramolecular electron-transfer steps, and to the lack of inhibitors that block the electron transfer at sites distinct from the substrate binding sites [6]. Many naturally occurring inhibitors of the complex are known, but these cannot be used for a quantitative structure–activity relationship (QSAR) study due to the limited number of known derivatives. Yet, the first QSAR studies on synthetic inhibitors modelling the ubiquinone binding site of the complex have been published [7]. These studies were complicated by the high hydrophobicity of substrate and inhibitors.

Recently we found that the fluorinated 1-*N*-arylamino-1-arylmethanephosphonic acid esters (**1**; see Scheme 1) represent a new class of uncouplers that selectively inhibit complex I in mitochondria at higher concentrations. Preliminary studies indicate that these compounds interact with complex I in a mode that is distinctly different from that of the hitherto known inhibitors. Several derivatives of the parent structure have been synthesized [8a]; the reaction sequences are shown in Scheme 2. In addition, heteroaryl-substituted compounds **6** and **7** were obtained by corresponding synthetic procedures; they are shown in

*To whom correspondence should be addressed.

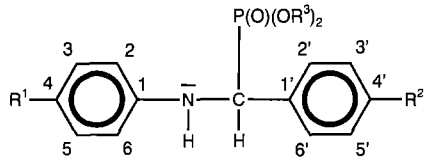

Scheme 1. General structure of 1-*N*-arylamino-1-arylmethanephosphonic esters.

Scheme 3. These compounds were tested together with compounds of type **1** and the precursor imine **4ab** (see Scheme 1) for their inhibitory effects. Conformational studies on these compounds have been supported by molecular modelling [8e–g] and NMR spectroscopy [8h]. Reflections on a series of calculated structures for 1-*N*-arylamino-1-arylmethanephosphonic acid esters afford information on the active binding sites of these inhibitors. The model presented here may help to understand the mode of binding between this new class of inhibitors and the key complex in respiration.

Methods

The respiratory activities were measured with bovine heart mitochondria using an oxygen electrode [6]. All molecular dynamics (MD) simulations and systematic conformational searches were performed with the program package QUANTA 3.3.1/CHARMm 2.2 [9]. The atomic partial charges were obtained with MOPAC 6.0 PM3 [10]. The main dihedral angles responsible for the molecular conformation, including rotations around the Ph-N, N-C, C-P and C-Ph axes, were analysed by systematic conformational searches (torsion increments, involving one or two dihedral angles simultaneously; 0° to 360°, in steps of 10°) and by MD simulations at two different temperatures (300 K and 700 K; simulation periods: 90 ps and 150 ps, respectively).

The geometrical optimizations following the conformational analysis were performed using the program MOPAC 6.0 PM3. PM3 was chosen because it comprises the hitherto best parameterization of phosphorus atoms for optimization of the molecular geometry and calculation of the heat of formation [11]. For interpretation of the electrostatic potential surfaces (so-called Connolly surfaces) with QUANTA 3.3.1, the data obtained by MOPAC 6.0/7.0 PM3 calculations were used. The molecular modelling studies were performed using the force field and the semiempirical software packages mentioned above, running on a Silicon Graphics INDY workstation and a Convex C220 computer.

Solvent effects were considered with CHARMm (15 Å sphere; $CHCl_3$) and VAMP 4.0 [12] PM3 (SCRF; cavity = 1.0; $CHCl_3$). The molecular structures simulated in a hypothetical gas phase and in a $CHCl_3$ solution do not show any significant differences. This is reasonable, since the 1-*N*-arylamino-1-arylmethanephosphonic acid esters are noncharged molecules and the solvent $CHCl_3$ has a low dielectric constant. $CHCl_3$ was used as a solvent in the simulations, since the ^1H NMR spectra were also obtained in $CDCl_3$ solutions.

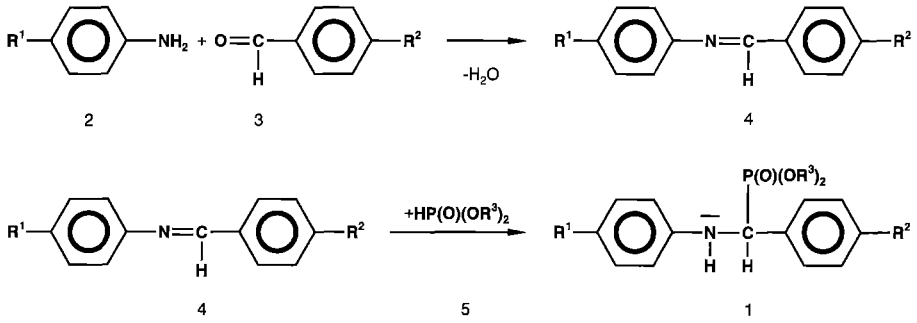

Compound	R^1	R^2	R^3	Compound	R^1	R^2	R^3
4aa	H	H		**1baa**	4-CF_3O	H	Me
4ab	H	CF_3O		**1bab**	4-CF_3O	H	Et
4ba	CF_3O	H		**1bac**	4-CF_3O	H	*i*-Pr
4bb	CF_3O	CF_3O		**1bad**	4-CF_3O	H	*n*-Bu
4be	CF_3O	$N(CH_3)_2$		**1bae**	4-CF_3O	H	Ph
4ca	CF_3	H		**1bbb**	4-CF_3O	4-CF_3O	Et
4cc	CF_3	CF_3		**1beb**	4-CF_3O	4-$N(CH_3)_2$	Et
4da	CH_3O	H		**1cab**	4-CF_3	H	Et
1aab	H	H	Et	**1ccb**	4-CF_3	4-CF_3	Et
1abb	H	4-CF_3O	Et	**1dab**	4-CH_3O	H	Et

Scheme 2. Formation of 1-*N*-arylamino-1-arylmethanephosphonic esters. **2,3**: R^1, R^2: (a) H; (b) CF_3O; (c) CF_3; (d) CH_3O; (e) $N(CH_3)_2$. **5**: R^3: (a) CH_3; (b) C_2H_5; (c) *i*-C_3H_7; (d) *n*-C_4H_9; (e) C_6H_5.

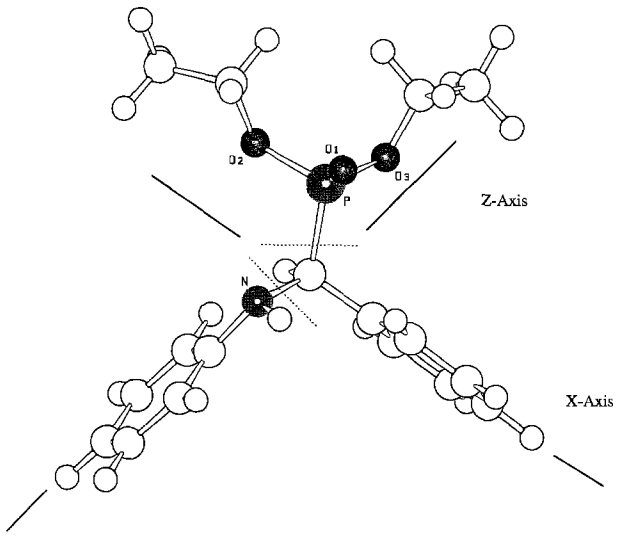

Fig. 1. N-H side view of the simulated molecular structure of **1aab**. The solid lines indicate the molecular axes; the dashed lines separate the three characteristic building blocks of the inhibitor molecule (see the text for details).

Results and Discussion

Structural aspects

Figure 1 shows the parent structure of 1-*N*-phenylamino-1-phenylmethanephosphonic acid diethyl ester, **1aab**. Since the methine carbon is chiral, we obtained racemic compounds via the synthesis presented above. Thus, two enantiomeric forms exist in solution. For simplicity only the (*S*)-configuration has been studied by conformational analysis, but it must be mentioned that all compounds were tested as racemic forms.

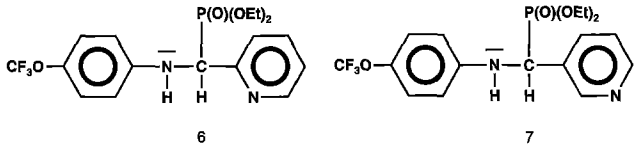

Scheme 3. Structures of heteroaryl-substituted compounds **6** and **7**.

The most important dihedral angle refers to the rotation around the C-P axis. Figure 1 shows the molecular structure corresponding to the global minimum of the potential energy, where a trans-position of the H-C-P=O group is found. The rotation around the C-P axis of **1aab** is hindered by a rotational barrier of 25.9 kcal/mol, as calculated from torsion forcing with CHARMm and MOPAC PM3. This high rotational barrier is consistent with ^{1}H NMR spectra of **1aab** and also of all related derivatives at room temperature [8]. Variable temperature NMR measurements in the range 23–90 °C did not indicate significant conformational changes for the H-C-P=O unit. Molecular dynamics simulations yielded a pronounced stability for the optimized conformation, shown in Fig. 1. Only small variations of 20° around the anti conformation for the H-C-P=O dihedral angle are allowed.

The H-C-N-H skeleton shows an anti conformation as well, in which the N-H bond is close to the plane of the phenyl ring connected to the nitrogen atom (H-N-C^1_{Ar}-C^6_{Ar} = 24.9°; N-C^1_{Ar}-C^6_{Ar}-H = −5.3°). However, the H-C-N-H unit is more flexible than the H-C-P=O skeleton, and the H-C-N-H dihedral angle varies within a larger range, i.e. ±40°.

The simulated structure of **1aab** exhibits a flattened pyramidal coordination for the nitrogen atom, which is in

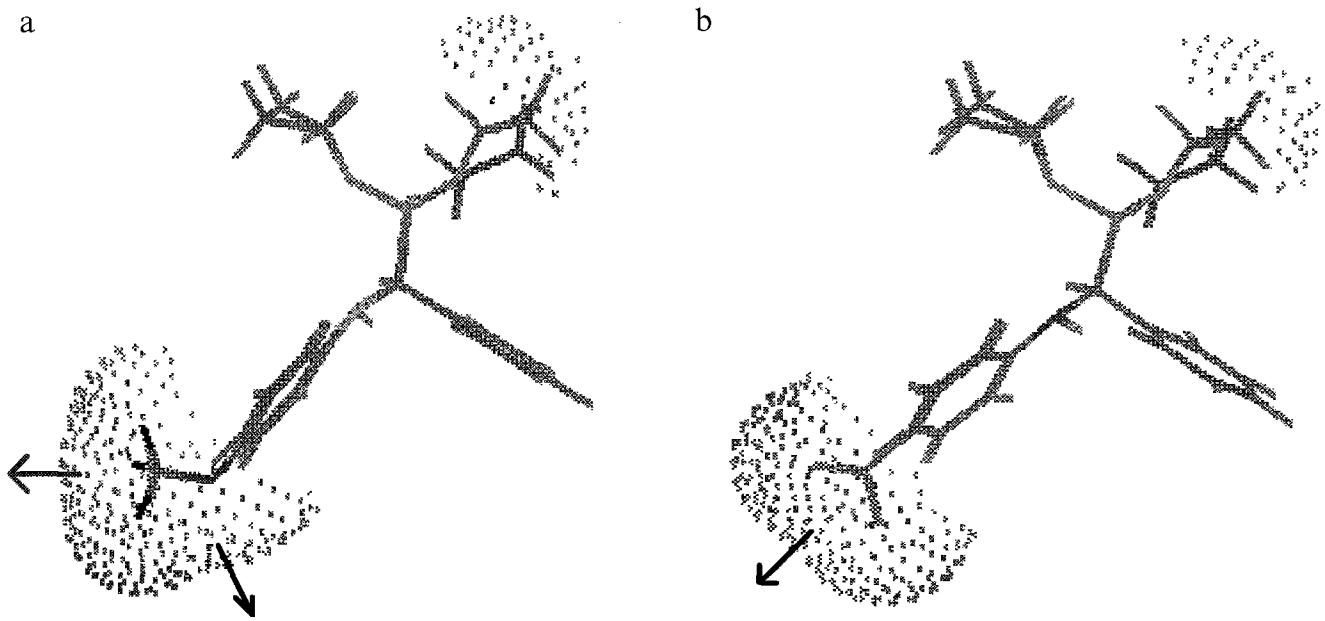

Fig. 2. Superpositions showing differences in the electrostatic potential surfaces. (a) **1aab** and **1bab**; (b) **1aab** and **1cab**.

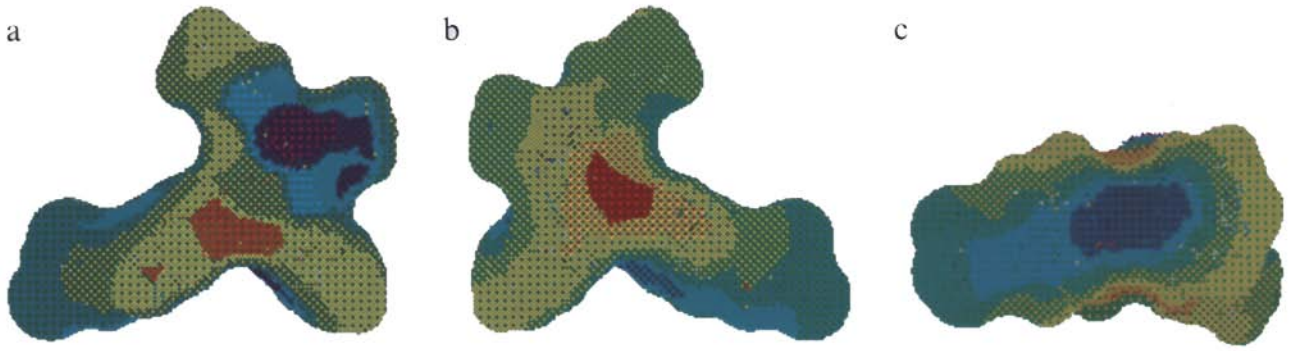

Fig. 3. Electrostatic potential distribution on the Connolly surface of **1bab**. Blue: negative electrostatic potential; red: positive electrostatic potential. (a) N-H side view (x,z plane); (b) C-H side view (x,z plane); (c) Ph-NH-CH-Ph bottom side view.

accordance with the solid-state structure [13; Belsky, V.K. and Finocchiaro, P., unpublished results]. The calculated C-N-C bond angle of 118.1° and the N-C^1_{Ar} bond length of 1.443 Å differ only slightly from the values found in the solid state (117.1° and 1.385 Å, respectively).

The phenyl ring planes are almost perpendicular to each other, with a corresponding angle of 98°. To illustrate their orientation further, we list some dihedral angles involving phenyl carbons: C^1_{Ar}-N-C-$C^{1'}_{Ar}$ = −85.6°; C^2_{Ar}-C^1_{Ar}-N-C = −31.4°; N-C-$C^{1'}_{Ar}$-$C^{6'}_{Ar}$ =−53.3°. The calculated orientation of the carbon-bound phenyl ring is consistent with the crystal structure, whereas the nitrogen-bound phenyl ring shows a slight deviation [13,14]. This can be explained by packing effects due to the formation of dimers in the solid state. This dimer effect is not taken into account in the simulations.

Substituent effects

The inhibitory effects of a series of 1-*N*-arylamino-1-arylmethanephosphonic acid esters interacting with complex I are listed in Table 1. The typical structure of 1-*N*-arylamino-1-arylmethanephosphonic acid esters may be divided into three regions, as shown in Fig. 1: (i) the *N*-arylamino group; (ii) the arylmethane group; and (iii) the phosphonic acid ester group with the P=O dipole. Some preliminary rules for correlations between structural units and activity may be derived from Table 1.

(i) The N-arylamino function (aniline unit) If R^3 = C_2H_5 and R^2 = H, then the activity will decrease with R^1 in the following order: $CF_3O > CF_3 > CH_3O$ (**1aab**, **1bab**, **1dab**). An approximate rule may be that the activity will increase with increasing group electronegativity in R^1. The inhibition maximum culminates in 1-(*N*-4-trifluoromethoxyphenyl)-amino-1-phenylmethanephosphonic acid diethyl ester, **1bab**.

(ii) The arylmethane function (benzyl unit) If R^3 = C_2H_5 and R^1 = H, then the activity will decrease with increasing group electronegativity of R^1, obviously reversing the polarity inside the inhibitor molecule (see data for **1aab** and **1abb**). An analogous trend is observed for a series having $R^3 = C_2H_5$ and $R^1 = CF_3$ (see **1cab** and **1ccb**). Most important are the observations made for $R^3 = C_2H_5$

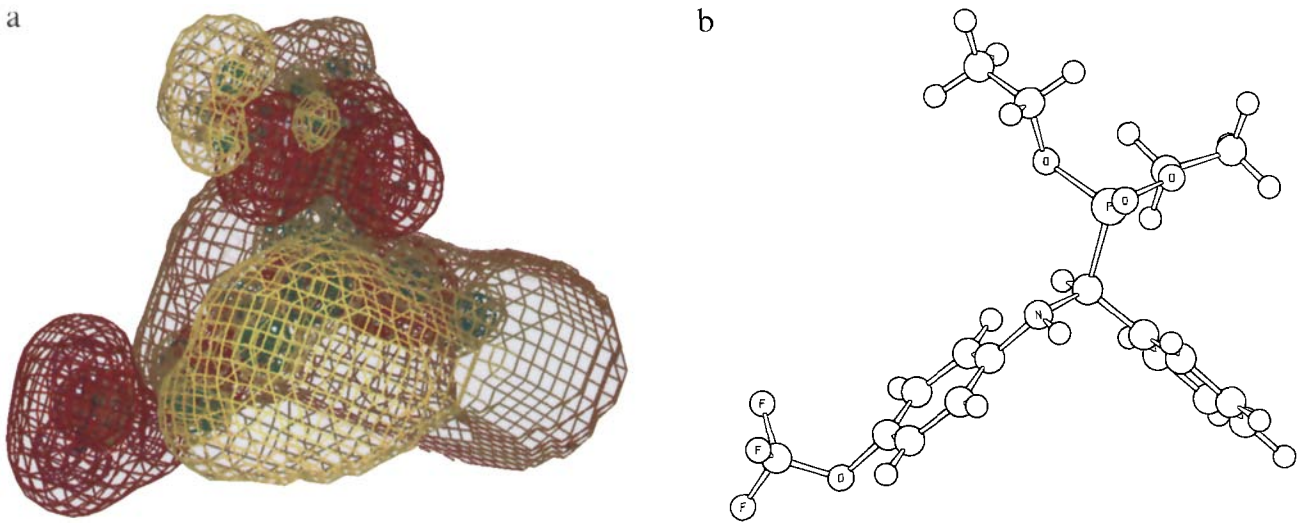

Fig. 4. (a) Probe-interaction simulation with a positively charged H^+. The red (yellow) coloured region shows zones with the highest (lowest) possibility for electrostatic interactions with positively charged partners. (b) Structure of **1bab** in an analogous orientation as shown in Fig. 4a.

and $R^1 = CF_3O$: the activities decrease drastically with R^2 in the order $H > N(CH_3)_2 > CF_3O$, as shown for compounds **1bab**, **6**, **7**, **1beb** and **1bbb**. While **1bab** is the most active of all compounds monitored in this series, up to now **1bbb** has been found to be virtually inactive. Exchanging C_6H_5 for the heteroaromatic pyridyl units 2-C_5H_4N or 3-C_5H_4N reduces the activity in the series **1bab**, **6**, **7**.

(iii) The phosphonic acid ester function Initially, for preparative reasons, the more easily accessible series of diethyl 1-*N*-arylamino-1-arylmethanephosphonates (**1aab**, **1abb**, **1bab**, **1cab**, **1dab**, **1bbb**, **1beb**, **1ccb**, **6** and **7**) was designed. Fortunately, the results presented in Table 1 show that a maximum of inhibitor activity is achieved with the diethyl ester **1bab**, while the corresponding dimethyl- (**1baa**), di-*iso*-propyl- (**1bac**) and di-*n*-butyl- (**1bad**) esters exhibit decreasing activities. The phosphonic acid ester unit is obviously essential for binding of the inhibitor to the enzyme. This may also be concluded from comparison of the activities of the nonphosphorylated Schiff base precursor **4ba** and the phosphorylated reaction product **1bab**.

Molecular modelling

The effects of substitution of the *para*-H by a CF_3O or a CF_3 group on the *N*-arylamino group of the parent structure **1aab** are visualized in Fig. 2, in which differences in the corresponding electrostatic potential surfaces are shown. The electronic and hydrophobic properties of the CF_3O and the CF_3 group are very similar, but CF_3O gives rise to better inhibition. Both groups generate comparable dipole moments and negative electrostatic potential surfaces, but the oxygen of the CF_3O fragment contains an additional electrostatic interaction vector directed along the x-axis at the CF_3O moiety, as shown in Fig. 2.

The CF_3O group has an electron-withdrawing effect, reaching as far as the phosphonic ester moiety: by substituting the *para*-hydrogen in **1aab** by 4-CF_3O, the P=O double-bond character in **1bab** is increased, while the electronic density at the phosphorus atom is decreased. This long-range substituent effect is supported by $^{31}P\{^1H\}$ NMR measurements [15] of a series of diphenyl 1-*N*-arylamino-1-arylmethanephosphonates. In addition, the exchange of H by CF_3O reverses the polarization along the z-axis (dipole moments along the z-axis: –0.23 D (**1aab**) and +1.88 D (**1bab**), respectively). The strongest dipole moment for the unsubstituted parent compound **1aab** results from the P=O group directed along the y-axis (–1.22 D). The strongest dipole moment for the trifluoromethoxy derivative **1bab** is directed along the z-axis, while the dipole along the y-axis is increased to –1.61 D. The total dipole moment has increased significantly, from 1.58 D (**1aab**) to 3.04 D (**1bab**). Due to this electron-withdrawing effect the CF_3O substituent induces a distinct change in the positive electrostatic potential surface near the N-H and C-H protons, as visualized in Fig. 3. This leads to an increase in possible intermolecular bonds or electrostatic interactions. Additional negative electrostatic potential surfaces are formed due to the presence of the oxygen and fluorine atoms.

Model of interaction sites

In order to obtain a model for potential sites of interaction between the 1-*N*-arylamino-1-arylmethanephosphonic acid esters and the protein, the molecular electrostatic potential (MEP) distribution on the Connolly surface of **1bab** was calculated, as shown in Fig. 3. The Connolly surface is defined as the molecular surface calculated at a distance of 1.4 Å beyond the van der Waals radii.

The bottom side view of the potential surface for the Ph-NH-CH-Ph moiety of structure **1bab** shows a decline in the positive electrostatic potential region in the aromatic ring planes and an expansion of the negative region in the middle of the molecule compared to **1aab**. For the description of the possible intermolecular bonds or electrostatic interactions of **1bab** a 'probe interaction simulation' was calculated for **1bab**, which is shown in Fig. 4a. With 'probe interaction', iso-electrostatic potential surfaces are defined in order to investigate the approach of a positive point charge (H^+) from all space directions to the target molecule. For an improved visualization, the molecular structure of **1bab** is shown in Fig. 4b, using a ball-and-stick projection in the identical orientation as in Fig. 3. The red regions show zones with attraction, whereas the yellow regions represent repulsive zones. From the probe interaction it is obvious that the oxygen

TABLE 1
INHIBITORY EFFECTS OF 1-*N*-ARYLAMINO-1-ARYLMETHANEPHOSPHONIC ACID ESTERS **1** ON COMPLEX I

Compound	R^1	R^2	R^3	K_{i50} (μM)
1bab	CF_3O	H	Et	26
1bac	CF_3O	H	*i*-Pr	38
1baa	CF_3O	H	Me	51
6	CF_3O	[a]	Et	51
1cab	CF_3	H	Et	61
4ba	CF_3O	H	[b]	63
7	CF_3O	[c]	Et	64
1aab	H	H	Et	78
1dab	CH_3O	H	Et	82
1bab	CF_3O	H	*n*-Bu	157
1abb	H	CF_3O	Et	185
1beb	CF_3O	$N(CH_3)_2$	Et	206
1ccb	CF_3	CF_3	Et	240
1bbb	CF_3O	CF_3O	Et	n.i.

Experimental inhibitory effects are denoted as K_{i50} (μM inhibitor at 50% inhibition); n.i. = no inhibition.
[a] 2-C_5H_4N-substituted compound **6**.
[b] Schiff base **4ba**, the nonphosphorylated precursor to **1bab**.
[c] 3-C_5H_4N-substituted compound **7**.

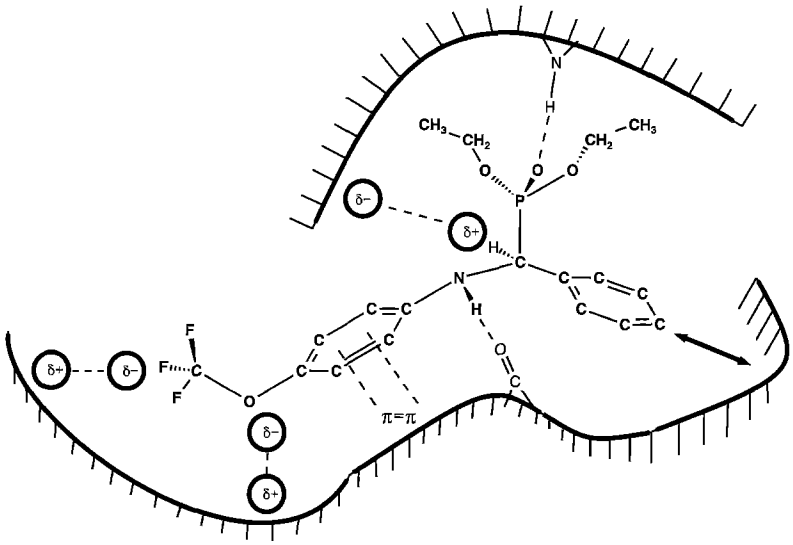

Fig. 5. Model for the description of the possible molecular electrostatic interactions of **1bab** with the enzyme binding site. H-bridges: δ+ - - - δ–: dipolar and charge–charge interaction; π=π: charge-transfer interaction; ← →: repulsive interaction.

atom and the fluorine atoms of the CF_3O group, the P=O oxygen atom and the bottom of the structure, with the aromatic Ph-NH-CH-Ph moiety, are preferred for the approach of a positive charge or polarized atoms. The fluorine atoms build up a prominent, nonshielded negative electrostatic potential for intermolecular interaction, as does the P=O oxygen. The negative electrostatic potential of the Ph-NH-CH-Ph moiety is only accessible from the lower side in this model. By contrast, a repulsive effect is caused by the aromatic, the N-H and the C-H protons in the plane of the phenyl rings. They represent regions with the highest positive electrostatic potential for electrostatic interactions like hydrogen bonds.

Conclusions

The electronic and steric effects caused by substitution of the parent structure **1aab**, as well as the information obtained from conformational analysis, permit the construction of a simple model for the binding site of compound **1bab**. Salient features caused by modifications of the parent structure shown in Fig. 1 confirm the division of the structure into three interaction regions, namely the *N*-arylamino group, the phosphonate group and the phenylmethane moiety.

The most sensitive moiety for the inhibitory effect of **1aab** is located at the N-CF_3O-phenylamino fragment, having a definite impact on the electronic properties of the molecule. The fluorine atoms are responsible for the specific binding ability, while there is a further increase of inhibitory power by insertion of the oxygen atom due to its additional electrostatic effect along the x-axis of the CF_3O group.

Significant features of the phosphonate region containing the P=O dipole stem from the bulky ester moiety, in which the ethyl group gives the best fit between the steric demands and the hydrophobic requirements. Furthermore, this region is marked by the electrostatic properties of the P=O group, allowing further intermolecular interactions like H-bridges.

The substitution at the aromatic ring of the phenylmethane group leads to an increase of steric demands, thus lowering the inhibitory effect. Increase of the electronic density at the phenylmethane group leads to a lower electronic density in the *N*-arylamino ring system, thereby raising the inhibitory power relative to the parent structure.

The ability to have electrostatic interactions is, in addition to the conformational and hydrophobic contributions, a characteristic feature of the inhibitory effect of compound **1bab**. The possible interactions of this compound with the unknown enzyme binding site are depicted in Fig. 5. This model accounts for the electrostatic interactions with the CF_3O, the P=O, the N-H and the C-H moieties, as well as for the charge-transfer interaction with the *N*-arylamino moiety and the repulsive effect of the phenylmethane part. Thus, a combination of conformational analysis and structure–activity data has been used to develop a simple model that explains the inhibitory effect of compound **1bab** on the NADH:ubiquinone oxidoreductase.

Acknowledgements

This study was supported by the Ministerium für Wissenschaft und Forschung des Landes Nordrheinwestfalen, which sponsored the Arbeitsgemeinschaft Fluorchemie NRW. Thanks are due to the Fonds der Chemischen Industrie for material support. Helpful discussions with Dr. R. Peters (Molecular Simulation Inc.) are acknowledged.

References

1 Weiss, H. and Friedrich, T., J. Bioenerg. Biomembranes, 23 (1991) 743.
2 Weiss, H., Friedrich, T., Hofhaus, G. and Preis, D., Eur. J. Biochem., 197 (1991) 563.
3 Walker, J.E., Q. Rev. Biophys., 25 (1992) 253.
4 Friedrich, T., Weidner, U., Nehls, U., Fecke, W., Schneider, R. and Weiss, H., J. Bioenerg. Biomembranes, 25 (1993) 331.
5 Wallace, D.C., Annu. Rev. Biochem., 61 (1992) 1175.
6 Friedrich, T., Van Heek, P., Leif, H., Ohnishi, T., Forche, E., Kunze, B., Janssen, R., Trowietzsch-Kienast, W., Höfle, G., Reichenbach, H. and Weiss, H., Eur. J. Biochem., 219 (1994) 691.
7 Oettmeier, W., Masson, K. and Soll, M., Biochim. Biophys. Acta, 1099 (1992) 262.
8 a. Hägele, G., Gruß, U. and Dronia, H., Phosphorus Sulfur Silicon, 77 (1993) 318.
b. Failla, S., Finocchiaro, P., Latronico, M. and Libertini, M., Phosphorus Sulfur Silicon, 88 (1994) 185.
c. Gruß, U. and Hägele, G., Phosphorus Sulfur Silicon, 97 (1994) 209.
d. Gruß, U., forthcoming Ph.D. Thesis, Heinrich-Heine-Universität Düsseldorf, Düsseldorf, Germany, 1996.
e. Dronia, H., Ph.D. Thesis, Heinrich-Heine-Universität Düsseldorf, Düsseldorf, Germany, 1995.
f. Spiske, R., Diplomarbeit Heinrich-Heine-Universität Düsseldorf, Düsseldorf, Germany, 1992.
g. Spiske, R., forthcoming Ph.D. Thesis, Heinrich-Heine-Universität Düsseldorf, Düsseldorf, Germany, 1996.
h. Orlovskii, V.V., Vovsi, B.A. and Zakharova, L.F., Zh. Obshch. Khim., 42 (1972) 1165.
9 MSI Molecular Simulation Ltd., Cambridge, U.K., 1994.
10 Stewart, J.J.P., J. Comput. Chem., 10 (1989) 209.
11 Stewart, J.J.P., J. Comput. Chem., 10 (1989) 221.
12 Clark, T., VAMP, Universität of Erlangen, Erlangen, Germany, 1990.
13 Ruzic, Z., Kojic-Prodic, B. and Sljwkic, M., Acta Crystallogr., B34 (1978) 3110.
14 Dronia, H., Failla, S., Finocchiaro, P., Gruß, U. and Hägele, G., Phosphorus Sulfur Silicon, 101 (1995) 149.
15 Smith, S.J., Zimmer, H., Fluck, E. and Fischer, P., Phosphorus Sulfur Silicon, 35 (1988) 105.